Plant Physiology and Biochemistry 220 (2025) 109466

Contents lists available at ScienceDirect

Plant Physiology and Biochemistry

journal homepage: www.elsevier.com/locate/plaphy

The reducing end of cell wall oligosaccharides is critical for DAMP activity in *Arabidopsis thaliana* and can be exploited by oligosaccharide oxidases in the reduction of oxidized phenolics

Moira Giovannoni [a,1], Anna Scortica [a,1], Valentina Scafati [a], Emilia Piccirilli [a,b], Daniela Sorio [c], Manuel Benedetti [a,*], Benedetta Mattei [a]

[a] Department of Life, Health and Environmental Sciences, University of L'Aquila, 67100, L'Aquila, Italy
[b] University School for Advanced Studies IUSS Pavia, Pavia, 27100, Italy
[c] Centro Piattaforme Tecnologiche, University of Verona, 37134, Verona, Italy

ARTICLE INFO

Keywords:
Oligosaccharide oxidase
DAMPs
Plant immunity
Guaiacol
Bi-phenoquinone
Cell wall metabolism

ABSTRACT

The enzymatic hydrolysis of cell wall polysaccharides results in the production of oligosaccharides with nature of damage-associated molecular patterns (DAMPs) that are perceived by plants as danger signals. The *in vitro* oxidation of oligogalacturonides and cellodextrins by plant FAD-dependent oligosaccharide-oxidases (OSOXs) suppresses their elicitor activity *in vivo*, suggesting a protective role of OSOXs against a prolonged activation of defense responses potentially deleterious for plant health. However, OSOXs are also produced by phytopathogens and saprotrophs, complicating the understanding of their role in plant-microbe interactions. Here, we demonstrate the oxidation catalyzed by specific fungal OSOXs also converts the elicitor-active cello-tetraose and xylotetraose into elicitor-inactive forms, indicating that the oxidation state of cell wall oligosaccharides is crucial for their DAMP function, irrespective of whether the OSOX originates from fungi or plants. In addition, we also found that certain OSOXs can transfer the electrons from the reducing end of these oligosaccharides to oxidized phenolics (bi-phenoquinones) instead of molecular O_2, highlighting an unexpected sub-functionalization of these enzymes. The activity of OSOXs may be crucial for a thorough understanding of cell wall metabolism since these enzymes can redirect the reducing power from sugars to phenolic components of the plant cell wall, an insight with relevant implications for plant physiology and biotechnology.

1. Introduction

Plant cell wall is an extracellular structure composed of polysaccharides, proteins and phenolic compounds. It plays a fundamental role in physiological processes, including the maintenance of turgor pressure, cell shape, and protection against microbes (Scortica et al., 2022). In addition, plant cell wall can also function as a reservoir of energy, with its reducing power locked within its complex architecture and heterogenous composition. To colonize the plant tissue, phytopathogens need first to break down the different components of the cell wall, whose degradation is achieved through the secretion of cell wall-degrading enzymes, a class of enzymes mainly constituted by glycosyl hydrolases, oxidoreductases and lyases (Giovannoni et al., 2020). The enzymatic hydrolysis of cell wall polysaccharides results in a transient accumulation of cell wall fragments with nature of damage-associated molecular patterns (DAMPs) such as oligogalacturonides (OGs) and cellodextrins (CDs), that plants perceive as danger signals (Pontiggia et al., 2020). These cell wall oligosaccharides may also act as negative regulators of various developmental processes. Their activity is crucial for balancing the growth-defense trade-off due to their contrasting effects on immunity and growth (Pontiggia et al., 2020; Scortica et al., 2022). It is important to bear in mind that, although DAMP-triggered immunity confers protection against invading microbes, an exaggerated and prolonged activation of defense negatively affects plant health. A clear effect of this process can be observed in the stunted growth-phenotype of *Arabidopsis thaliana* plants that accumulate OGs in uncontrolled manner (Benedetti et al., 2015). *In vitro*, the oxidation of OGs and CDs by plant FAD-dependent oligosaccharide-oxidases (OSOXs) strongly reduces their elicitor activity, suggesting a

* Corresponding author.
E-mail address: manuel.benedetti@univaq.it (M. Benedetti).
[1] These authors equally contributed to this work.

https://doi.org/10.1016/j.plaphy.2024.109466
Received 17 September 2024; Received in revised form 27 December 2024; Accepted 28 December 2024
Available online 2 January 2025

Abbreviations:

ABTS 2,2′-azino-bis-(3-ethylbenzothiazoline-6-sulfonic acid)
BBE-l Berberine Bridge Enzyme-like
CDs cellodextrins
DAMPs damage-associated molecular patterns
EIC extracted ion chromatogram
FAD flavin adenine dinucleotide
(FHS-)CELLOX1 (sumoylated flag-his tagged) cellodextrin-oxidase 1 (cellodextrin: oxygen oxidoreductase, EC number: 1.21.3.3)
Flg22 flagellin 22 oligopeptide
G/TGm guaiacol/tetra-guaiacol mixture
(H-)GOOX (his-tagged) gluco-oligosaccharide oxidase (gluco-oligosaccharide:oxygen oxidoreductase, EC number: 1.21.3.3)
(H-)XOOX (his-tagged) xylo-oligosaccharide oxidase (xylo-oligosaccharide:oxygen oxidoreductase, EC number: 1.21.3.3)
HRP horseradish peroxidase VI-A type (phenolic donor: hydrogen-peroxide oxidoreductase, EC number: 1.11.1.7)
MAPK mitogen-activated protein kinase
OGs oligogalacturonides
OGOX1 oligogalacturonide-oxidase 1 (oligogalacturonide:oxygen oxidoreductase, EC number: 1.21.3.3)
OSOX oligosaccharide oxidase
(ox-)CD4 (oxidized) cello-tetraose
(ox-)Xyl4 (oxidized) xylo-tetraose
POD peroxidase (phenolic donor: hydrogen-peroxide oxidoreductase, EC number: 1.11.1.7)
PRR pattern recognition receptor
Q-TOF LC/MS quadrupole time-of-flight liquid chromatography/mass spectrometry
TGm tetra-guaiacol mixture

protective role of OSOXs against a self-deleterious hyper-activation of DAMP-triggered immunity (Benedetti et al., 2018; Costantini et al., 2024; Locci et al., 2019). In accordance with this hypothesis, Arabidopsis plants treated with oxidized OGs and CDs showed a lower defense gene induction, a weaker oxidative burst, and a reduced accumulation of callose compared to plants treated with the corresponding not oxidized elicitors (Benedetti et al., 2018; Costantini et al., 2024; Locci et al., 2019). OSOXs belong to the family of berberine bridge enzyme-like (BBE-l) proteins, a class of flavoenzymes widely distributed in bacteria, fungi and plants (Daniel et al., 2017). Different OSOXs from *A. thaliana* have been identified as specific oligogalacturonide-oxidases (OGOXs) and cellodextrin-oxidases (CELLOXs) (Benedetti et al., 2018; Costantini et al., 2024; Locci et al., 2019). OGOXs include four isoforms (OGOX1-4) that oxidize OGs, whereas CELLOXs include two isoforms (CELLOX1-2) that oxidize CDs. Interestingly, OSOXs are also produced by phytopathogens and saprotrophs such as the gluco-oligosaccharide oxidase from *Sarocladium strictum* (GOOX) (Lee et al., 2005), active on CDs as plant CELLOXs, and the xylo-oligosaccharide oxidase from *Miceliophtora thermophila* (XOOX), active on xylo-oligosaccharides (Ferrari et al., 2016). Thus, the existence of OSOXs in both fungi and plants complicates the comprehension of their role in plant-microbe interaction. In the last 20 years, the different OSOXs so far identified have been described as specific oxidases, i.e., oxidoreductases capable of transferring electrons from the reducing end of oligosaccharides to molecular O_2, thereby producing H_2O_2. According to the stoichiometry of enzymatic reaction, one molecule of H_2O_2 is produced for each C1-oxidized oligosaccharide. However, in the presence of short oligosaccharides and specific electron acceptors, both OGOX1 and CELLOX1 also act as conditional dehydrogenase, for example, by transferring the electrons from the reducing end of tetra-galacturonic acid (OG4) and cello-tetraose (CD4), respectively, to the radical cation $ABTS^{\bullet+}$ rather than to molecular O_2 (Scortica et al., 2023). This enzymatic feature makes the reaction catalyzed by OSOX challenging to predict *in vivo*. The oxidation of oligosaccharides may lead to the production of H_2O_2 or other compounds, depending on factors such as the polymerization degree of oligosaccharide elicitors, the extracellular concentration of O_2 and the availability of other potential electron acceptors (Benedetti et al., 2018; Pontiggia et al., 2020; Scortica et al., 2023). The complexity is further increased by the presence of multiple OSOX paralogs within the same organism (e.g. OGOX1-4, CELLOX1,2). Notably, both *cellox1* null mutant and CELLOX1-overexpressing plants exhibited an increased resistance to *Botrytis cinerea* infection, highlighting the limitations of conventional genetic approaches in elucidating the role of OSOXs in plant immunity (Locci et al., 2019; Costantini et al., 2024).

Recently, 3-α-L-arabinofuranosyl-xylo-tetraose and xylo-tetraose (Xyl4) have been reported to act as DAMPs in *A. thaliana* (Fernández-Calvo et al., 2024; Mélida et al., 2020). By using OSOXs of both fungal and plant origin, we demonstrate here that oxidized Xyl4 (xylo-tetraonic acid, ox-Xyl4) and oxidized CD4 (cello-tetraonic acid, ox-CD4) have a weaker elicitor activity than their not oxidized counterparts, reinforcing the view that DAMP action of cell wall oligosaccharides is dependent on the oxidation state of their reducing end, regardless whether the OSOX employed for their oxidation originates from fungi or plants. In addition, we also prove that certain OSOXs redirect the electrons from the reducing end of cell wall oligosaccharides to bi-phenoquinones, i.e., a class of oxidized phenolics, instead of molecular O_2. This sub-functionalization, based on the preference for different electron acceptor substrates (e.g., O_2 *vs* bi-phenoquinones), could explain the presence of multiple OSOX paralogs with similar sugar oxidizing activities within the same organism (Benedetti et al., 2018; Costantini et al., 2024).

2. Materials and methods

2.1. Design of the constructs expressing plant and fungal OSOXs in Pichia pastoris

The sumoylated-flag-his tagged form of cellodextrin-oxidase 1 from *A. thaliana* (FHS-CELLOX1) was obtained according to (Costantini et al., 2024; Scortica et al., 2022). The gene encoding the fungal OSOXs i.e., the xylo-oligosaccharide oxidase (XOOX) from *M. thermophila* C1 and the gluco-oligosaccharide oxidase (GOOX) from *S. strictum*, were codon-optimized according to the codon usage of *Komagataella phaffii*, formerly known as *Pichia pastoris*, using the software OPTIMIZER (http://genomes.urv.es/OPTIMIZER/) (Puigbò et al., 2007). The putative signal peptides of both fungal OSOXs were identified by using the SignalP-5.0 server (http://www.cbs.dtu.dk/services/SignalP/) (Almagro Armenteros et al., 2019) and were excluded from the gene design. The two sequences were synthesized by Genescript (https://www.genscript.com/) and then were cloned in pPICZαB (Invitrogen, San Diego, CA) in frame with the sequences encoding the 6xHis-tag (HHHHHH) and the yeast α factor signal peptide.

2.2. Preparation of oxidized Xyl4 (ox-Xyl4) and oxidized CD4 (ox-CD4)

Commercial Xyl4 (O-XTE, Megazyme) or CD4 (O-CTE, Megazyme) was dissolved in 20 mM Tris-HCl pH 7.0 and 20 mM NaCl or, alternatively, in ultrapure H_2O (0.4-2 $mg.mL^{-1}$). The mixture was incubated at 30 °C for 16 h by adding the purified OSOX (0.04 $g.L^{-1}$), i.e., H-XOOX for Xyl4, H-GOOX or FHS-CELLOX1 for CD4, and catalase (0.02 $g.L^{-1}$)

from bovine liver (Sigma). After incubation, a small aliquot of each reaction was analyzed by HPLC to verify the oxidation state of Xyl4 and CD4. HPLC analysis was performed with the same instrumentations and conditions described in (Scafati et al., 2022) by modifying the amount of sugar standards used in the analysis (2 mg.mL^{-1}) and the volume injection of each sample (5 μL). All the data acquired were processed by Shimadzu LabSolutions control software. The final reactions were loaded into a Vivaspin® 500 (10000 MWCO PES) and then centrifuged (5 min, 4000×*g*) to separate OSOXs and catalase from the oxidized sugars. The filtrated sugars were quantified by using the total sugar assay (Dubois et al., 1956) and the reducing sugar assay (Lever, 1972). As controls, the same procedures were carried out on Xyl4 and CD4 by adding heat inactivated OSOXs and catalase.

2.3. MAPKs immunoblot analysis

10-day-old *A. thaliana* seedlings were treated with different oligosaccharide elicitors (80 μg.mL^{-1} each), i.e., Xyl4, ox-Xyl4 (H-XOOX), CD4, ox-CD4 (H-GOOX), ox-CD4 (FHS-CELLOX1), and with flg22 (10 nM) as positive control, for 5 and 10 min respectively. 20 seedlings (about 100–200 mg FW) were pulverized in liquid nitrogen and the total proteins were extracted with 100 μl of phosphatase-inhibiting buffer for 20 min (4 °C) and then centrifuged at 13000×*g* for 30 min (4 °C), in accordance with (Giovannoni, Marti, et al., 2021). The supernatant was recovered, and the protein extracts (40 μg for each sample) were separated using 10% SDS-PAGE. For detection of phosphorylated MAPKs, the anti-p44/42-ERK antibody (1:2000, Cell Signaling Technology), which recognizes the double-phosphorylated activation loop of MAPKs in the TEY motif (Ichimura et al., 2002; Zhang and Dong, 2007), was used. For detection of total MAPKs, the anti-AtMPK3 (1:2500, Sigma, M8318) and anti-AtMPK6 (1:10000, Sigma, A7104) antibodies were used. Nitrocellulose membranes were then incubated in Tris-buffered saline, 0.1% Tween 20 and 0.5% (w/v) BSA with a secondary horseradish peroxidase-(POD)-conjugated anti-rabbit antibody (1:6000, Bio-Rad). The chemiluminescence-based detection was performed by using the Clarity™ Western ECL substrate detection kit (Bio-Rad) in accordance with (Giovannoni, Lironi et al., 2021). The signal intensities were quantified by using the ImageJ software (LOCI, University of Wisconsin) and the obtained values were used to assess the phosphorylation percentage (%), calculated through the following formula: [(intensity of α-P44/42 signal upon treatment with oxidized tetra-saccharide - intensity of α-P44/42 signal upon treatment with buffer): (intensity of α-P44/42 signal upon treatment with not oxidized tetra-saccharide - intensity of α-P44/42 signal upon treatment with buffer)] * 100%. For treatments with not oxidized tetra-saccharides (Xyl4, CD4), the intensity of the α-P44/42 signal resulting from treatment with buffer was subtracted from the intensity of α-P44/42 signal resulting from treatment with the not oxidized tetra-saccharide and normalized to 100%.

2.4. RNA extraction and gene expression analysis

10-day-old seedlings were treated with each oligosaccharide-based elicitor (80 μg.mL^{-1}), i.e., [Xyl4, ox-Xyl4 (H-XOOX), CD4, ox-CD4 (H-GOOX), ox-CD4 (FHS-CELLOX1), and flg22 (10 nM) for 1 h. Plant tissues were grinded with Retsch MM 301 vibratory mill for 1 min at 24 Hz. NucleoZOL one phase RNA purification reagent was used to extract the total RNA from samples following the manufacturer's specification. The cDNA synthesis and quantitative real-time PCR (qRT-PCR) analyses were performed in accordance with (Giovannoni, Lironi, et al., 2021). The gene expression analysis was performed on three different biological replicates (each composed of three technical replicates) by mediating the results obtained. The primers used for qRT-PCR analysis are listed in Supplementary Table S1.

2.5. Botrytis cinerea infection assay

The fungus *Botrytis cinerea* was grown on MEP medium [malt-agar 2% (w/v), peptone 1% (w/v) and micro-agar 1.5% (w/v)] until sporulation and then it was maintained at 20 °C in a dark chamber in accordance with (Giovannoni, Larini, et al., 2021). The infection assays were performed in accordance with (Giovannoni et al., 2024). In brief, for elicitor-induced protection, plants were sprayed with water, Xyl4, ox-Xyl4 (H-XOOX), CD4, ox-CD4 (FHS-CELLOX1, H-GOOX) (200 μg.mL^{-1} each), flg22 (1 μM) and colloidal chitin (100 μg.mL^{-1}) 24 h before fungal infection (2.5 * 10^6 spores for each inoculation site). *B. cinerea* infection was assessed 48–72 h after inoculation by measuring the lesion areas (mm^2) of infected leaves by using the ImageJ software (https://imagej.nih.gov/ij).

3. Results

3.1. Heterologous expression of plant and fungal OSOXs and preparation of oxidized tetra-saccharides

We expressed FHS-CELLOX1, the his-tagged version of GOOX (H-GOOX) and the his-tagged version of XOOX (H-XOOX) in *K. phaffii* – formerly known as *P. pastoris* (Heistinger et al., 2020). CELLOX1 and GOOX are both active on CDs whereas XOOX is active on xylo-oligosaccharides (Ferrari et al., 2016; Lee et al., 2005; Locci et al., 2019). FHS-CELLOX1 and H-XOOX were purified from the culture filtrate of recombinant yeasts by using a 6xhis-tag affinity chromatography. As already reported (Lee et al., 2005), the Ni-column was not able to bind H-GOOX, therefore its purification was carried out by using a hydrophobic interaction chromatography (HIC). The quality of purified FHS-CELLOX1, H-XOOX and H-GOOX was assessed by SDS-PAGE and immuno-decoration analyses (Fig. 1a). Subsequently, the purified FHS-CELLOX1 and H-GOOX were separately used to oxidize CD4 whereas H-XOOX was used to oxidize Xyl4. Cello- and xylo-tetramers served as reference cell wall oligomers with a proven elicitor activity in *A. thaliana* (Fernández-Calvo et al., 2024; Locci et al., 2019). The enzymatic reactions also occurred in the presence of a mammalian catalase, here used to remove the hydrogen peroxide generated by oligosaccharide oxidation and recycle the molecular oxygen back to the reaction (Pontiggia et al., 2020; Scortica et al., 2022). Following the enzymatic reactions, the oxidized tetra-saccharides were firstly checked by HPLC analysis and then were quantified by colorimetric assays (Fig. 1b and c). In accordance with our previous analysis (Scortica et al., 2023), neutral oligosaccharides, once oxidized, strongly bound to the Pb-affinity column and, differently from their not oxidized counterparts, could not be eluted by a isocratic gradient (Fig. 1b and c-*left*). An ultra-filtration step allowed to separate OSOXs and catalase from the oxidized sugars that, in turn, were evaluated by two different colorimetric assays (Dubois et al., 1956; Lever, 1972). Following the *in vitro* oxidation, the sugar preparations showed a significant change in the [total sugars: reducing sugars] ratio, increasing from an initial value of 4.35 ± 0.15 to a final value of 32.5 ± 3.5. This shift clearly indicated a drastic decrease in the number of reducing ends (Fig. 1b and c-*right*). Based on these values, we estimated an average oxidation yield greater than 86.5%, calculated as 100% – [100: (32.5 : 4.35)]%. In accordance with previous results from (Vuong et al., 2013; Ferrari et al., 2016; Locci et al., 2019), mass spectrometry analysis of enzymatic products confirmed that oxidation occurred at the reducing end of each tetra-saccharide. Oxidized products were xylo-tetraonic acid (ox-Xyl4) for the reaction catalyzed by H-XOOX, and cello-tetraonic acid (ox-CD4) for the reactions catalyzed by H-GOOX and FHS-CELLOX1 (Supplementary Fig. S1). In conclusion, the pure OSOXs (Fig. 1a) were successfully used to obtain two different mixtures of ox-CD4 [ox-CD4 (H-GOOX), ox-CD4 (FHS-CELLOX1)] and one mixture of ox-Xyl4 [ox-Xyl4 (H-XOOX)] (Fig. 1b and c).

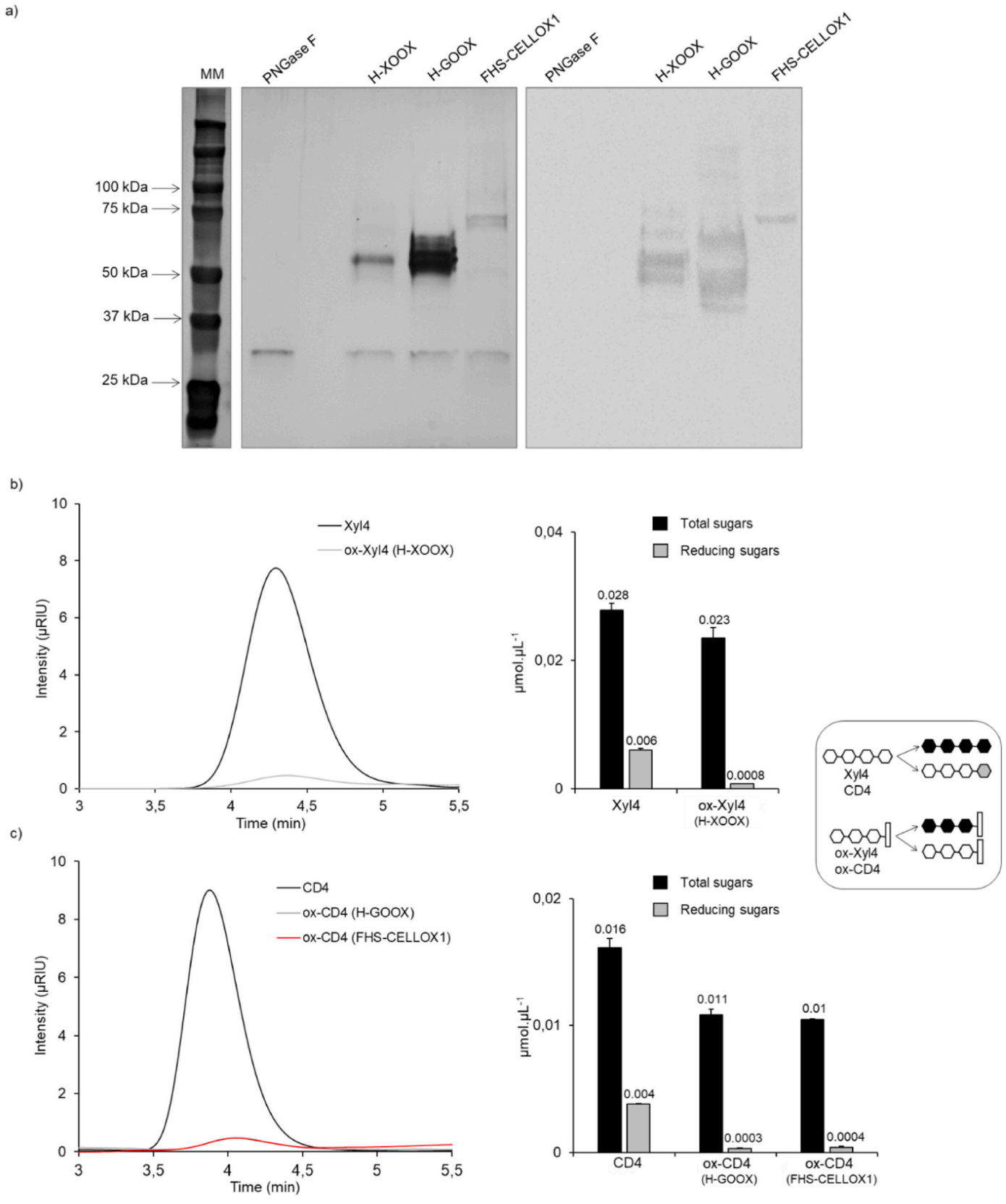

(caption on next page)

Fig. 1. Oxidized oligosaccharides produced by recombinant plant and fungal OSOXs. a) *Left*, SDS-PAGE/silver nitrate staining analysis of purified OSOXs upon PNGase F treatment. Molecular weight marker (MM) is also reported. *Right*, immuno-decoration analysis of the same samples shown on the left by using an antibody directed against the 6xhis tag. b) *Left*, chromatographic analysis and (*right*) quantification of total and reducing sugars carried out on a Xyl4 preparation before (Xyl4) and after incubation with H-XOOX [ox-Xyl4 (H-XOOX)]. c) *Left*, chromatographic analysis and (*right*) quantification of total and reducing sugars carried out on a CD4 preparation before (CD4) and after incubation with H-GOOX [ox-CD4 (H-GOOX)] or with FHS-CELLOX1 [ox-CD4 (FHS-CELLOX1)]. b,c) The sugar units detected as total (black) and reducing sugars (grey) are indicated for each untreated (Xyl4 and CD4) and enzymatically-treated (ox-Xyl4, ox-CD4) tetra-saccharide in the box on the right. Here, the C1-oxidized unit (aldonic acid) is represented as a rectangle. Xyl4 and CD4 were used as reference. Values are mean ± SD (n = 3). For a clearer interpretation, mean is reported on the top of each bar. [CD4, cello-tetraose; FHS-CELLOX 1, flag-his-sumoylated cellodextrin oxidase 1; H-GOOX, his-gluco-oligosaccharide oxidase; H-XOOX, his-xylo-oligosaccharide oxidase; ox-CD4, oxidized cello-tetraose; ox-Xyl4, oxidized xylo-tetraose; PNGase F, Peptide:N-glycosidase F; Xyl4, xylo-tetraose].

3.2. Plant defense responses are induced to a lesser extent by oxidized tetra-saccharides regardless of the type of OSOX used for their oxidation

To check whether ox-Xyl4 and ox-CD4 are still active as elicitors, we investigated three early defense responses (i.e., MAPK activation, extracellular accumulation of H_2O_2 and defense marker gene induction) on Arabidopsis seedlings treated with the oligosaccharide preparations shown in (Fig. 1b and c). Here, the pathogen-associated molecular pattern (PAMP) flg22 was used as positive control (Giovannoni, Lironi, et al., 2021; Giovannoni, Marti, et al., 2021) (Fig. 2). The phosphorylation status of MPK3/6 in elicitor-treated seedlings was examined by an immuno-decoration analysis at 5 and 10 min from each treatment, since MAPK activation occurs rapidly and coincides with the earliest observable responses triggered by DAMPs/PAMPs perception (Nühse et al., 2000; Galletti et al., 2011). Compared to the treatment with Xyl4 and CD4, the phosphorylation status of MPK3/6 in seedlings treated with the oxidized tetra-saccharides was lower than 65% (ox-Xyl) or almost absent (ox-CD4) at both time-points analyzed, indicating that oxidized oligomers were worse elicitors than their not oxidized counterparts (Fig. 2a). Notably, the entity of such a decreased phosphorylation was similar in the seedlings treated with ox-CD4 (H-GOOX) and ox-CD4 (FHS-CELLOX1) (Fig. 2a). The extracellular accumulation of H_2O_2 was measured in the culture medium of seedlings treated with the same oligosaccharide preparations by using the xylenol orange assay (Benedetti et al., 2018). Upon elicitor-treatment, the accumulation of H_2O_2 was 2-fold lower in the culture medium of seedlings treated with ox-Xyl4 and ox-CD4 (Fig. 2b). Also in this case, the decrease of H_2O_2 accumulation was almost comparable in the seedlings treated with ox-CD4 (H-GOOX) and ox-CD4 (FHS-CELLOX1) (Fig. 2b). Interestingly, this analysis also highlighted different kinetics of extracellular H_2O_2 accumulation between PAMP- and DAMP-treated plants since the extracellular accumulation of H_2O_2 was bi-phasic (30 and 90 min) and mono-phasic (30 min), respectively, for flg22-and oligosaccharide-treated seedlings (Fig. 2b). The expression level of four defense-related genes known to be induced by OGs, CDs and flg22 was analyzed by qRT-PCR, namely *FOX1* (At1g26380), *CYP81F2* (AT5G57220), *FRK1* (AT2G19190) and *WRKY33* (AT2G38470) which generally peak at around 1 h after elicitation (Costantini et al., 2024; Galletti et al., 2008; Gravino et al., 2017) (Fig. 2c). Compared to the treatment with Xyl4 and CD4, plants treated with oxidized elicitors exhibited reduced induction of all investigated genes, confirming that oxidized oligosaccharides are less effective elicitors (Fig. 2). This holds true regardless of their chemical composition (i.e., 1,4-β-linked-xylose or -glucose) or the OSOX used for their *in vitro* oxidation, whether fungal H-GOOX or plant FHS-CELLOX1 (Fig. 1). To further evaluate the efficacy of oxidized oligosaccharides as plant elicitors, the basal and elicitor-induced resistance against the necrotrophic fungus *B. cinerea* was assayed by analyzing the leaf lesions caused by the fungus on the oligosaccharide-sprayed plants (Fig. 3). Pre-treatment with OGs or flg22 is known to promote protection against *B. cinerea* in Arabidopsis plants (Giovannoni et al., 2024). This protection results from the induction of a 'primed' state, that enhances the plants' responsiveness to subsequent exogenous challenges (Conrath, 2011; Martinez-Medina et al., 2016). To investigate the priming effect, the tetra-saccharides (Xyl4, CD4), the corresponding oxidized counterparts (ox-Xyl4, ox-CD4), and the microbial elicitors flg22 and chitin, both used as positive controls, were sprayed on adult plants. After 24 h, the treated leaves were inoculated with *B. cinerea* spores. Compared to flg22-, chitin-, Xyl4-and CD4-treated leaves, the treatment with ox-Xyl4 and ox-CD4 conferred a weaker protection against *B. cinerea* infection. These findings confirm the reduced efficacy of oxidized tetra-saccharides as plant elicitors (Fig. 3).

In conclusion, Xyl4 and CD4 effectively triggered MAPK activation, extracellular H_2O_2 accumulation and defense marker gene induction in seedlings, as well as an increased resistance against *B. cinerea* infection in the leaves of adult Arabidopsis plants. In contrast, ox-Xyl4 and ox-CD4 exhibited weak or negligible elicitor activity, regardless of the specific type of OSOX used for their *in vitro* oxidation (Figs. 2 and 3). Notably, ox-CD4 and ox-Xyl4 retained some residual elicitor activity (Figs 2 and 3), which may be attributed to incomplete *in vitro* oxidation (Fig. 1b and c-*right*).

3.3. The reducing end of cell wall tetra-saccharides can be exploited by H-XOOX and FHS-CELLOX1 in the reduction of oxidized phenolics

The existence of OSOXs in both plants and microbes makes the comprehension of their physiological role not easily inferable (Daniel et al., 2017; Pontiggia et al., 2020). *In vitro*, for example, the OSOX orthologs H-GOOX and FHS-CELLOX1 were both able to convert a DAMP (CD4) into a molecule with null elicitor activity (ox-CD4) in *A. thaliana* by concomitantly producing H_2O_2 (Figs. 1 and 2). The scenario becomes even more complex when we consider that both plants and fungi express OSOXs during their interaction (Pontiggia et al., 2020). To further investigate this aspect, we analyzed the different redox propensities of H-XOOX, H-GOOX and FHS-CELLOX1 in an attempt to highlight differences that were not evident in previous analyses (Costantini et al., 2024; Ferrari et al., 2016; Lee et al., 2005; Locci et al., 2019; Scortica et al., 2022, 2023). Given that (i) the plant cell wall is primarily composed of polysaccharides and polyphenols, and (ii) OSOXs function in the extracellular environment, their ability to transfer electrons from cell wall oligosaccharides to plant phenolics was investigated. As potential phenolic electron acceptor substrate, we used tetra-guaiacol, a tetra-phenolic compound obtained by the POD-catalyzed oxidative polymerization of the coniferyl alcohol analogue "guaiacol" (Supplementary Fig. S2). First, we determined the amount of each OSOX generating a similar H_2O_2 rate in the presence of equimolar concentration (50 μM) of appropriate tetra-saccharide (Fig. 4a). Then, these enzyme amounts were separately incubated in a reaction buffer containing a [guaiacol: tetra-guaiacol] mixture and POD. The assay, referred to as TG-reduction assay, included a concentration of tetra-guaiacol (~150 μM) similar to that of dissolved oxygen in ultrapure water (180–380 μM). This was done to provide OSOXs with an equal likelihood of transferring electrons from the C1-end of each tetra-saccharide to either molecular O_2 or tetra-guaiacol (Gray, 2002). The simultaneous presence of guaiacol and tetra-guaiacol in the reaction, at an approximate molar ratio of 4:1, facilitated the identification of the redox propensity of each OSOX and prevented the masking effect that could occur if only one phenolic species was present (Scortica et al., 2023). Surprisingly, the brownish color of the solution, typically attributed to tetra-guaiacol, decreased over time in the presence of two out of three OSOX/tetra-saccharide combinations (Supplementary

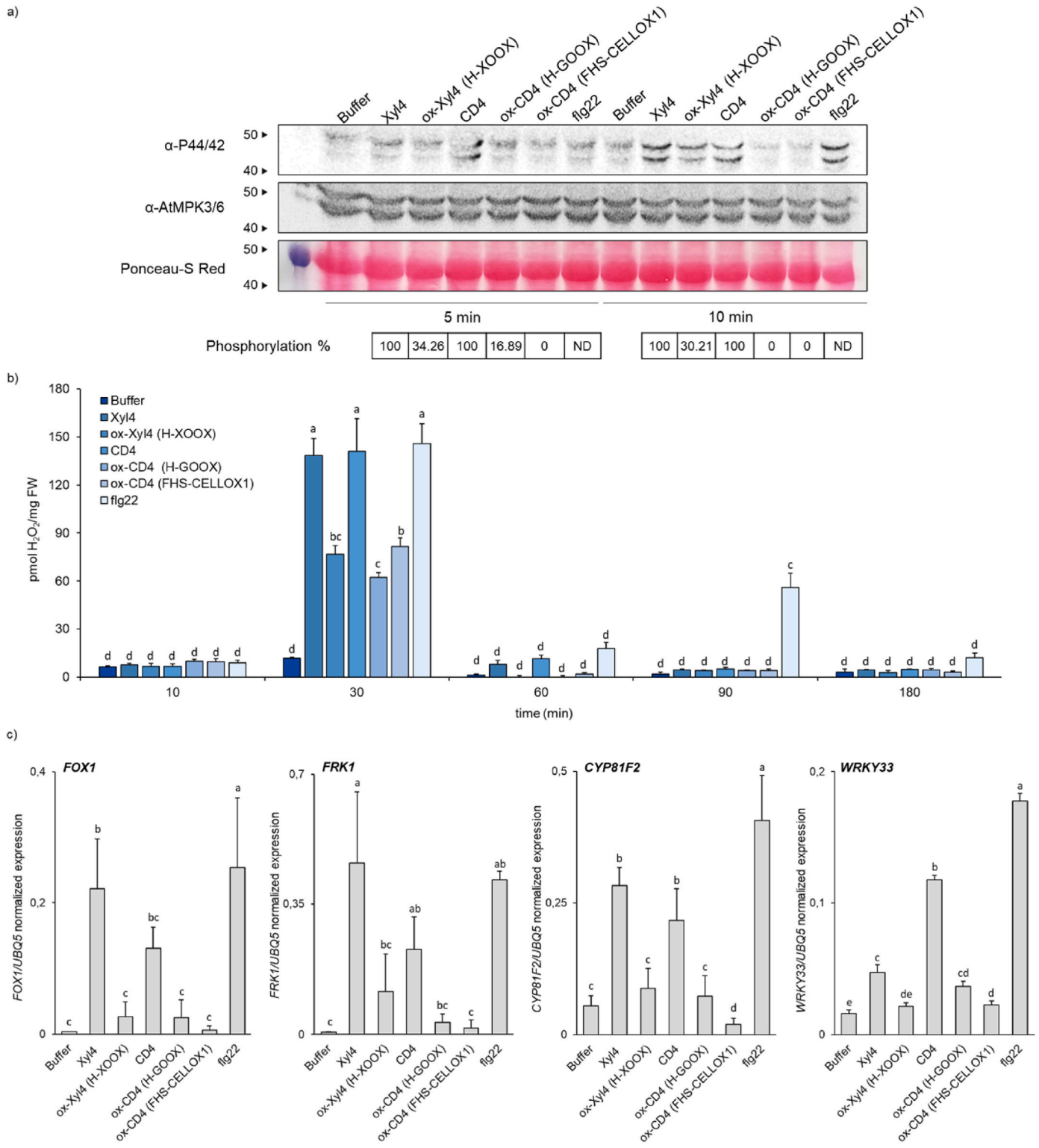

Fig. 2. Activation of early defense responses is reduced in Arabidopsis seedlings treated with oxidized oligosaccharides. a) Immunoblot analysis on MPK3/6 phosphorylation in 10-day-old wild type seedlings after 5 and 10 min-treatment with not oxidized and oxidized tetra-saccharides. Ponceau-S Red staining was used to verify the equal loading. Phosphorylation (%) refers to the relative quantification (%) of each signal intensity. ND, not determined. b) H_2O_2 accumulation at the indicated time-points as determined by xylenol orange assay in the growth medium of 10-day-old wild type seedlings after treatments with not oxidized and oxidized tetra-saccharides. Values represent mean ± SE (n = 5). c) Expression of the defense marker genes *FOX1*, *FRK1*, *CYP81F2* and *WRKY33* by qRT-PCR in 10-day-old wild type seedlings after 1h-treatment with not oxidized and oxidized tetra-saccharides. Normalization of gene expression was performed by using *UBQ5* as reference. Bars represent mean ± SD (n = 3). Treatments with the reaction buffer alone (buffer) and with flg22 were used as negative and positive controls, respectively. Significant differences were determined using one-way ANOVA followed by Tukey's HSD post hoc test ($p < 0.05$). Values sharing the same letters are not significantly different. [CD4, cello-tetraose; FHS-CELLOX 1, flag-his-sumoylated cellodextrin oxidase 1; flg22, flagellin 22 oligopeptide; H-GOOX, his-gluco-oligosaccharide oxidase; H-XOOX, his-xylo-oligosaccharide oxidase; ox-CD4, oxidized cello-tetraose; ox-Xyl4, oxidized xylo-tetraose; Xyl4, xylo-tetraose]. (For interpretation of the references to color in this figure legend, the reader is referred to the Web version of this article.)

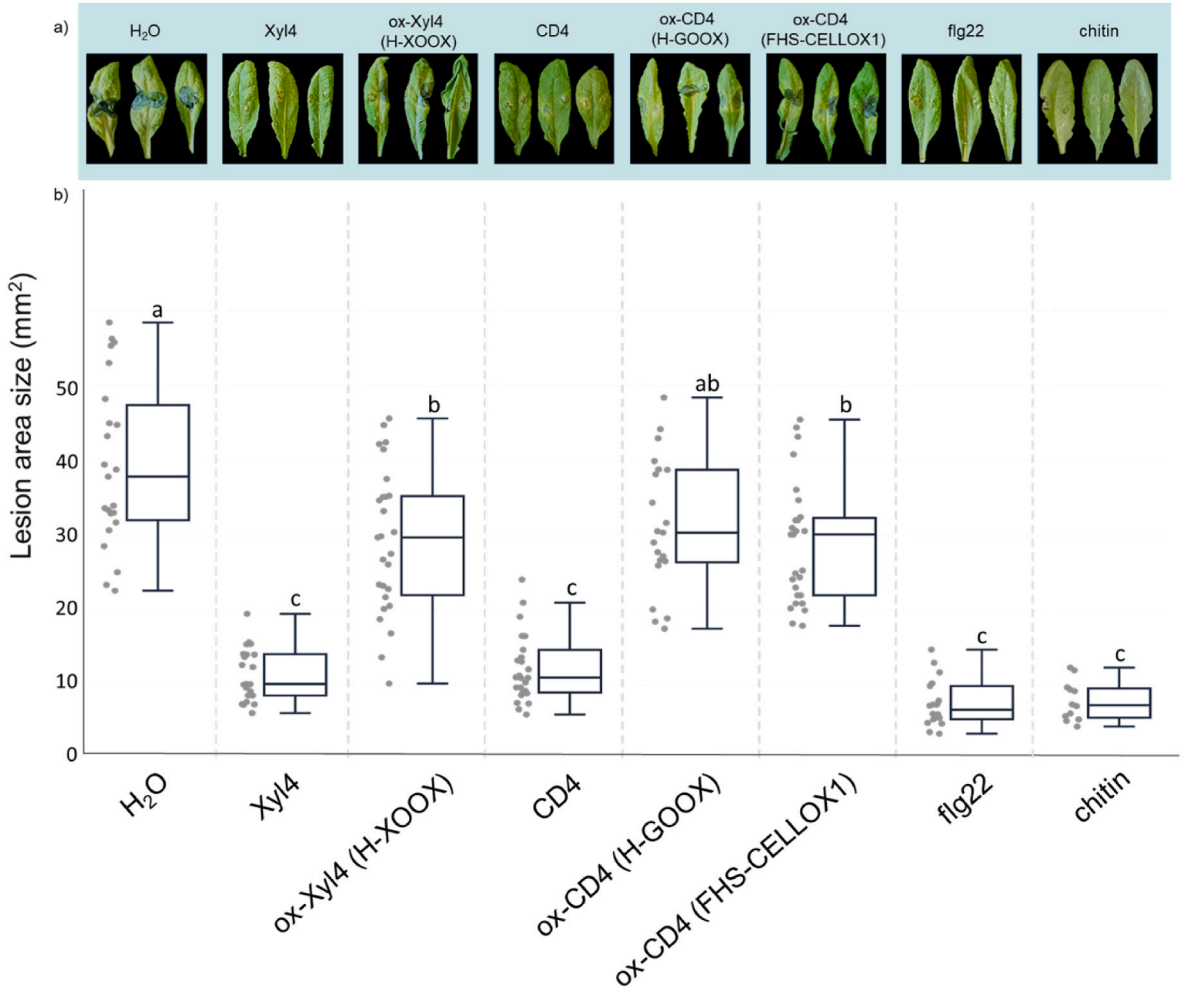

Fig. 3. Elicitor-induced protection against *B. cinerea* is reduced in Arabidopsis plants treated with oxidized oligosaccharides. a,b) *B. cinerea* infection assay was performed on the leaves of 4-week-old Arabidopsis plants after a pre-treatment with not oxidized, oxidized tetra-saccharides, flg22 and chitin, 24 h before fungal inoculation. a) Representative images of infected Col-0 leaves and of (b) their lesion areas (mm^2) as measured 48 h post inoculation (hpi). The box plot shows the median and the corresponding data points of each pretreatment. Significant differences were determined using one-way ANOVA followed by Tukey's HSD post hoc test ($p < 0.05$). Values sharing the same letters are not significantly different. The experiment was repeated twice with similar results.

Fig. S3). In particular, the H-XOOX/Xyl4 and FHS-CELLOX/CD4 combinations displayed, respectively, a 10- and 1.3-fold higher discoloration activity than H_2O_2-generating activity, whereas the H-GOOX/CD4 combination did not display any discoloration effect (Fig. 4a and b). Based on these results, we demonstrated that OSOXs with seemingly similar substrate specificities (i.e., H-GOOX and FHS-CELLOX1) actually catalyze different reactions.

The discoloration activity of H-XOOX/Xyl4 and FHS-CELLOX1/CD4 combinations was more pronounced in a reaction buffer predominantly composed of tetra-guaiacol, i.e., with a [guaiacol: tetra-guaiacol] ratio in favor of tetra-guaiacol (Supplementary Movie S1). The absorption spectra obtained during these enzymatic reactions were consistent with our previous results but also provided additional insight (Fig. 4c and d). In the presence of H-XOOX/Xyl4 and FHS-CELLOX1/CD4 combinations, the double absorption peak generally attributed to tetra-guaiacol (at 423 and 475 nm) was markedly reduced after 10 min of reaction, whereas a new double absorption peak appeared at shorter wavelengths (266 and 292 nm) (Fig. 4c and d). This double absorption peak indicated that the reaction product(s) resulting from the discoloration activity of the OSOX/oligosaccharide pair were distinct from the starting substrate, i.e., guaiacol (which has a single absorption peak at 280 nm) (Fig. 4c and d). However, the addition of fresh H_2O_2 to the exhausted reactions (i.e., when the tetra-saccharides had been fully oxidized by OSOXs) restored the double absorption peak typically associated with tetra-guaiacol. This clearly demonstrated that the product(s) generated by POD served as substrate(s) for OSOXs, and vice versa (Fig. 4c and d).

Supplementary video related to this article can be found at https://doi.org/10.1016/j.plaphy.2024.109466

The same enzymatic reactions were further analyzed using a Q-TOF LC/MS system. Although the guaiacol used as a reference could not be detected, LC/MS successfully identified tetra-guaiacol as the $[M + H]^+$ adduct with a m/z of 489. Two different bi-phenoquinones were also detected as the $[M + H]^+$ adducts with a m/z of 245 (dimethoxy-bi-phenoquinone) and of 367 (hydroxy-methoxyphenyl-dimethoxy-bi-phenoquinone) in accordance with (Tonami et al., 2004; Hwang et al., 2008) (Supplementary Fig. S4). As expected, these molecular masses (m/z 245, 367 and 489) were specifically detected in the reaction containing guaiacol and POD only after the addition of H_2O_2 (Supplementary Fig. S4). The extracted ion chromatograms (EICs) for the hydroxy-methoxyphenyl-dimethoxy-bi-phenoquinone and tetra-guaiacol displayed distinct elution peaks, indicating the presence of different isomers for each oligomer (Supplementary Figs. S4b and c-*left panel*). Notably, bi-phenoquinones are compounds characterized by an amber color and absorption at 470 nm (Tonami et al., 2004;

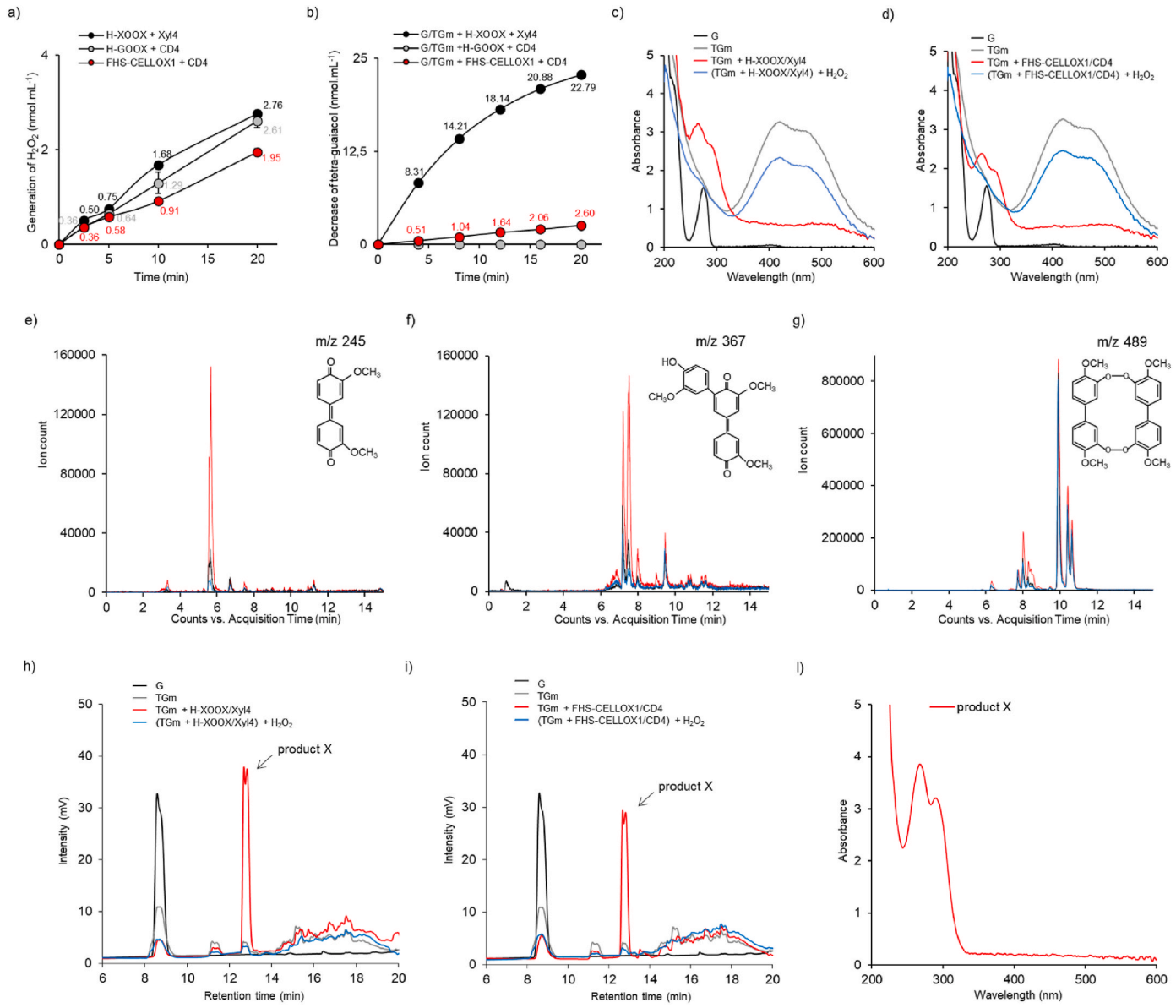

Fig. 4. The reducing end of cell wall oligosaccharides can be exploited by OSOXs in the reduction of oxidized phenolics. a) H_2O_2-generating and (b) tetra-guaiacol-discoloration activity, the latter expressed as decrease of tetra-guaiacol over time, at pH 5.0 by H-XOOX/Xyl4, H-GOOX/CD4 and FHS-CELLOX1/CD4 combinations as determined by the xylenol orange and TG-reduction assay, respectively. a, b) The reactions were performed using different concentrations of H-XOOX (740 nM), H-GOOX (1.5 nM) and FHS-CELLOX1 (4 nM) in the presence of each appropriate tetra-saccharide and (b) a [guaiacol: tetra-guaiacol] mixture. Values are mean ± SD (n = 3). For a clearer interpretation, mean is reported for each data-point. c, d) Changes in the UV/Visible absorption of tetra-guaiacol mixture 10-min after the addition of (c) H-XOOX/Xyl4 and (d) FHS-CELLOX1/CD4, and after the addition of fresh H_2O_2 (600 μM) to the exhausted enzymatic reactions. e-g) EIC of three different ions as detected in the starting tetra-guaiacol mixture (red line) and 10-min after the addition of H-XOOX/Xyl4 (blue line) and FHS-CELLOX1/CD4 (black line). The ion masses under investigation were characterized by a m/z of (e) 245, (f) 367 and (g) 489. Mass ions were mainly detected as $[M+H]^+$ adducts. For each ion, a hypothetical structure is reported. h, i) HPLC analysis of the reaction before (G) and after the addition of H_2O_2 (TGm), 10-min after the addition of (h) H-XOOX/Xyl4 and (i) FHS-CELLOX1/CD4 to TGm, and after the addition of fresh H_2O_2 (600 μM) to the exhausted enzymatic reactions. l) UV/Visible absorption of purified product X. a-i) The experiments were repeated three times with similar results. [CD4, cello-tetraose; FHS-CELLOX 1, flag-his-sumoylated cellodextrin oxidase 1; EIC, extracted ion chromatogram, G, guaiacol; G/TGm, (guaiacol: tetra-guaiacol) mixture, H-XOOX, his-xylo-oligosaccharide oxidase; OSOXs, oligosaccharide oxidases; POD, horseradish peroxidase type VI; TGm, tetra-guaiacol mixture; Xyl4, xylo-tetraose]. (For interpretation of the references to color in this figure legend, the reader is referred to the Web version of this article.)

Hwang et al., 2008). The activity of XOOX/Xyl4 and FHS-CELLOX1/CD4 combinations on the mixture suppressed all these species in a size-dependent manner: dimethoxy-bi-phenoquinone was suppressed more efficiently than hydroxy-methoxyphenyl-dimethoxy-bi-phenoquinone, which was in turn suppressed more efficiently than tetra-guaiacol, with the latter being suppressed to a lesser extent (Fig. 4e–g). This trend may be dependent not only on a more favorable redox potential of smaller molecules, which might fit more effectively into the active site of OSOXs, but also on the absence of exposed ketone groups in the tetra-guaiacol structure, pointing to this functional group as the main target for OSOX suppressing activity (Supplementary Fig. S4). These results corroborate recent findings reported by (Scortica et al., 2023), which demonstrated that different OSOX/short oligosaccharide combinations exhibit strong scavenging activity towards the radical cation $ABTS^{\bullet+}$. On the other hand, the missed detection of "suppressed/hydrogenated" di- and tri-guaiacol aligns with the Q-TOF

LC/MS system's inability to detect the guaiacol used as reference. Therefore, at this stage, we could not clearly determine whether the suppression of bi-phenoquinones by OSOXs involved only their reduction or also their depolymerization into guaiacol.

To deeper investigate this aspect, the same enzymatic reactions were also analyzed by HPLC chromatography. This technique was employed to measure the amount of guaiacol at three different time-points of enzymatic reaction, i.e., before and after the addition of H_2O_2, and 10 min after the addition of H-XOOX/Xyl4 and FHS-CELLOX1/CD4 combinations to the tetra-guaiacol mixture (Fig. 4h and i). In the presence of H_2O_2, POD oxidized most of the starting guaiacol but the newly formed oligomers, i.e., bi-phenoquinones and tetra-guaiacol, were not clearly detected. The addition of H-XOOX/Xyl4 and FHS-CELLOX1/CD4 combinations to the tetra-guaiacol mixture slightly decreased the amount of residual guaiacol, an effect ascribable to a weak production of H_2O_2 by OSOXs and that POD, in turn, used to oxidize a small amount of the remaining guaiacol (Fig. 4h and i). The activity of OSOXs also led to a notable accumulation of an unidentified compound, hereafter referred to as product "X", which was characterized by a double elution peak with a retention time of 12.7–12.8 min, significantly longer than that of guaiacol, which eluted at 8.6 min (Fig. 4h and i). After the addition of fresh H_2O_2 to the exhausted reactions, such compound was quickly oxidized by POD (Fig. 4h and i), confirming that the products generated by POD served as substrates for OSOXs, and vice versa (Fig. 4c,d,h,i). These results demonstrated that the activity of OSOXs on the tetra-guaiacol mixture did not catalyze any depolymerization into guaiacol (Fig. 4h and i), and indicated that the major products of their activity are hydrogenated compounds, i.e., plausibly oligo-guaiacols (Fig. 4c–i). As further validation, the product "X" was purified by HPLC and checked by UV/Vis absorption (Fig. 4l), and then was analyzed by Orbitrap LC-MS (Supplementary Fig. S5). Intriguingly, the UV/Vis spectrum of purified product X was characterized by a double absorption peak comparable to that obtained from OSOX activities as shown in Fig. 4c and d (Fig. 4l). LC-MS analysis of product X revealed the presence of an ion mass compatible with tri-guaiacol (m/z 369), i.e., the hydroxylated form of hydroxy-methoxyphenyl-dimethoxy-bi-phenoquinone (Fig. 4f–l; Supplementary Fig. S5). The missed detection of di-guaiacol (m/z 247), i.e., the hydroxylated form of dimethoxy-bi-phenoquinone, may be ascribed to its fast conversion into tri-guaiacol by POD, a hypothesis strongly supported by the concomitant consumption of guaiacol during OSOX activity (Fig. 4h and i).

By integrating the results obtained from the different analyses (UV/Visible absorption, HPLC, LC-MS), we concluded the oligosaccharide-dependent discoloration activity of OSOXs mainly consisted of a reducing activity on bi-phenoquinones to form oligo-phenols (Supplementary Fig. S6).

4. Discussion

We demonstrate that C1-oxidized cell wall oligosaccharides lose their ability to function as DAMPs in *A. thaliana*, irrespective of whether OSOX used for their *in vitro* oxidation is of plant or microbial origin. It is likely that the open-chain acid residue at the C1-end may impair binding with plant recognition receptors (PRRs), highlighting the reducing end as critical for oligosaccharide-receptor interactions (Fernández-Calvo et al., 2024). It is also possible that, in addition to PRR-mediated recognition, the signal transduction cascade triggered by a cell wall DAMP may require its oxidation. Although various mutant plants impaired in cell wall DAMP perception have been described (Fernández-Calvo et al., 2024; Giovannoni et al., 2024; Tseng et al., 2022), a mutant plant exhibiting a completely null response to a cell wall DAMP has never been isolated, supporting the idea that cell wall DAMP-mediated signaling may involve multiple pathways. It is worth noting that C1-oxidized oligosaccharides used to treat plants have been usually prepared *in vitro* (Benedetti et al., 2018; Costantini et al., 2024; Locci et al., 2019), preventing endogenous OSOXs from using them as an *in vivo* electron source. Consequently, plant response triggered by *in vitro*-oxidized oligosaccharides is inevitably partial (Spiro et al., 1998; Benedetti et al., 2018; Locci et al., 2019; Costantini et al., 2024).

Dimethoxy-bi-phenoquinones can be produced through the oxidative polymerization of guaiacol by both plant and fungal peroxidases (Tonami et al., 2004; Hwang et al., 2008), and this explains why plant and fungal OSOXs are both active on them (Supplementary Figure S4, Fig. 4e–g). During the microbial hydrolysis of cell wall polysaccharides, the oligosaccharide-dependent reducing activity of OSOXs may serve as a strategy for regenerating phenolic compounds and lowering the concentration of extracellular H_2O_2 (Scortica et al., 2023). In accordance with this hypothesis, the bi-phenoquinones suppressed by XOOX and CELLOX1 were re-oxidized by PODs through the consumption of additional H_2O_2 (Fig. 4c,d,h,i). In our experimental conditions, H_2O_2-generating and discoloration activities of H-GOOX were almost comparable in the [guaiacol: tetra-guaiacol] mixture, resulting in no clear net activity (Fig. 4b, Supplementary Fig. S3b). To understand the biological significance of this result, it is worth bearing in mind that the virulence of certain fungal pathogens, such as *Botrytis cinerea*, is enhanced by the accumulation of reactive oxygen species (ROS) in plant tissues (Rolke et al., 2004). In this scenario, a fungal OSOX with higher reducing activity than H_2O_2-generating activity may be counter-productive for a successful infection. Indeed, the redox propensity of each fungal OSOX is closely related to the specific lifestyle and infection strategy of its microbial producer.

Fungal oligosaccharide oxidases belong to the CAZy (Carbohydrate Active Enzymes database, http://www.cazy.org/) (Drula et al., 2022) AA7 family (Auxiliary Activity Family 7). Several characterized AA7 oxidases feature a bi-covalently attached FAD cofactor via cysteine and histidine, similar to the Arabidopsis BBE-l oxidases, although plant enzymes are not currently classified within the AA7 family (Momeni et al., 2021). It is noteworthy however, that the type of active site and oxygen reactivity motif are not identical between XOOX, GOOX and CELLOX1 (Supplementary Fig. S7) (Mattevi, 2006). A deeper biochemical and structural characterization of plant OSOXs will be fundamental to identify the different metabolites acting as electron acceptors *in vivo* (Leferink et al., 2009; Zafred et al., 2015). Oxidation by a FAD-dependent enzyme typically follows a Ping-Pong Bi-Bi mechanism: one substrate enters the active site, transfers a hydride to the flavin, and then is released. Subsequently, a second molecule forms a complex to re-oxidize the flavin (Daniel et al., 2017). However, the radical cation scavenging activity of OGOX1 occurs mainly in the presence of short OGs, indicating that the substrate steric hindrance, along with their redox potential, influences the dual scavenging/oxidase activity of OSOXs (Scortica et al., 2023).

In conclusion, the finding that fungal OSOXs also oxidize cell wall oligosaccharides, thereby inactivating their DAMP activity (Fig. 2), suggests that the role of OSOXs in plant-microbe interaction is highly complex and extends beyond a potential involvement in DAMP homeostasis that is solely beneficial to plants (Benedetti et al., 2018; Pontiggia et al., 2020; Costantini et al., 2024). In this study, a novel role for OSOXs as metabolic connectors between the glucidic and phenolic components of plant cell wall has been uncovered. OSOXs with similar oligosaccharide-oxidizing activities can catalyze distinctly different reactions due to their varying abilities to redirect the reducing power from cell wall oligosaccharides to oxidized phenolics (Fig. 4). The latter is an additional sub-functionalization feature that might explain the co-presence of vary OSOX paralogs in the same organism (Daniel et al., 2017; Pontiggia et al., 2020). Due to their different redox propensities, OSOXs can either enhance or counteract the activity of metallo-enzymes on phenolic compounds, suggesting the existence of a complex network of enzymatic activities that has not been fully clarified so far (Herzog et al., 2019). In addition to offering essential insights into the comprehension of cell wall metabolism, advances in deciphering these processes will also pave the way to the application of OSOXs in green technologies and synthetic biology.

CRediT authorship contribution statement

Moira Giovannoni: writing – original draft, visualization, methodology, investigation, formal analysis, data curation. **Anna Scortica:** writing – original draft, visualization, methodology, investigation, formal analysis, data curation. **Valentina Scafati:** visualization, methodology, investigation. **Emilia Piccirilli:** visualization, methodology, investigation. **Daniela Sorio:** visualization, methodology, formal analysis. **Manuel Benedetti:** conceptualization, writing – review & editing, writing – original draft, visualization, supervision, methodology, investigation, formal analysis, data curation, funding acquisition, project management. **Benedetta Mattei:** writing – review & editing, supervision, methodology, formal analysis, funding acquisition, project management.

Declaration of competing interest

The authors declare that they have no known competing financial interests or personal relationships that could have appeared to influence the work reported in this paper.

Acknowledgements

The authors gratefully acknowledge “Centro Piattaforme Tecnologiche” (University of Verona, Italy) for support and assistance in mass spectrometry analysis. This work was supported by the Italian Ministry of University and Research (PRIN2022 – PNRR P2022TPZW3, funded to M.B.; PRIN 2022WLZ4HB and PRIN2022 – PNRR P2022KLXEC, both funded to B.M.) and the University of L’Aquila (Progetti di Ateneo 2023 – H_2O_2-BBE, funded to M.B.), and by the Italian national inter-university PhD course in Sustainable Development and Climate change.

Appendix B. Supplementary data

Supplementary data to this article can be found online at https://doi.org/10.1016/j.plaphy.2024.109466.

Data availability

All relevant data are included in the article and/or its Appendix B Supplementary data file. The data sets used and/or analyzed during the current study are available from the corresponding author on reasonable request.

References

Almagro Armenteros, J., Tsirigos, K., Sønderby, C., Petersen, T., Winther, O., Brunak, S., Nielsen, H., 2019. SignalP 5.0 improves signal peptide predictions using deep neural networks. Nat. Biotechnol. 37 (4). https://doi.org/10.1038/s41587-019-0036-z.

Benedetti, M., Pontiggia, D., Raggi, S., Cheng, Z., Scaloni, F., Ferrari, S., De Lorenzo, G., 2015. Plant immunity triggered by engineered in vivo release of oligogalacturonides, damage-associated molecular patterns. Proc. Natl. Acad. Sci. USA 112 (17), 5533–5538. https://doi.org/10.1073/pnas.1504154112.

Benedetti, M., Verrascina, I., Pontiggia, D., Locci, F., Mattei, B., De Lorenzo, G., Cervone, F., 2018. Four Arabidopsis berberine bridge enzyme-like proteins are specific oxidases that inactivate the elicitor-active oligogalacturonides. Plant J. : Cell Mole. Biol. 94 (2). https://doi.org/10.1111/tpj.13852.

Conrath, U., 2011. Molecular aspects of defence priming. Trends Plant Sci. 16 (10), 524–531. https://doi.org/10.1016/j.tplants.2011.06.004.

Costantini, S., Benedetti, M., Pontiggia, D., Giovannoni, M., Cervone, F., Mattei, B., De Lorenzo, G., 2024. Berberine bridge enzyme-like oxidases of cellodextrins and mixed-linked b-glucans control seed coat formation. Plant Physiol. 194 (1), 296–313. https://doi.org/10.1093/plphys/kiad457.

Daniel, B., Konrad, B., Toplak, M., Lahham, M., Messenlehner, J., Winkler, A., Macheroux, P., 2017. The family of berberine bridge enzyme-like enzymes: a treasure-trove of oxidative reactions. Arch. Biochem. Biophys. 632, 88–103. https://doi.org/10.1016/j.abb.2017.06.023.

Drula, E., Garron, M., Dogan, S., Lombard, V., Henrissat, B., Terrapon, N., 2022. The carbohydrate-active enzyme database: functions and literature. Nucleic Acids Res. 50 (D1). https://doi.org/10.1093/nar/gkab1045.

Dubois, M., Gilles, K.A., Hamilton, J.K., Rebers, P.A., Smith, F., 1956. Colorimetric methods for determination of sugars and related substances. Anal. Chem. 28, 350–358. https://doi.org/10.1021/ac60111a017".

Fernández-Calvo, P., López, G., Martín-Dacal, M., Aitouguinane, M., Carrasco-López, C., González-Bodí, S., Molina, A., 2024. Leucine rich repeat-malectin receptor kinases IGP1/CORK1, IGP3 and IGP4 are required for arabidopsis immune responses triggered by β-1,4-D-Xylo-oligosaccharides from plant cell walls. Cell surface 11. https://doi.org/10.1016/j.tcsw.2024.100124. Amsterdam, Netherlands.

Ferrari, A.R., Rozeboom, H.J., Dobruchowska, J.M., van Leeuwen, S.S., Vugts, A.S., Koetsier, M.J., Fraaije, M.W., 2016. Discovery of a xylooligosaccharide oxidase from *Myceliophthora thermophila* C1. J. Biol. Chem. 291 (45), 23709–23718. https://doi.org/10.1074/jbc.M116.741173.

Galletti, R., Denoux, C., Gambetta, S., Dewdney, J., Ausubel, F.M., De Lorenzo, G., Ferrari, S., 2008. The AtrbohD-mediated oxidative burst elicited by oligogalacturonides in Arabidopsis is dispensable for the activation of defense responses effective against *Botrytis cinerea*. Plant Physiol. 148 (3), 1695–1706. https://doi.org/10.1104/pp.108.127845.

Galletti, R., Ferrari, S., De Lorenzo, G., 2011. Arabidopsis MPK3 and MPK6 play different roles in basal and oligogalacturonide- or flagellin-induced resistance against *Botrytis cinerea*. Plant Physiol. 157 (3), 804–814. https://doi.org/10.1104/pp.111.174003.

Giovannoni, M., Gramegna, G., Benedetti, M., Mattei, B., 2020. Industrial use of cell wall degrading enzymes: the fine line between production strategy and economic feasibility. Front. Bioeng. Biotechnol. 8. https://doi.org/10.3389/fbioe.2020.00356.

Giovannoni, M., Larini, I., Scafati, V., Scortica, A., Compri, M., Pontiggia, Mattei, B., 2021a. A novel *Penicillium sumatraense* isolate reveals an arsenal of degrading enzymes exploitable in algal bio-refinery processes. Biotechnol. Biofuels 14 (1). https://doi.org/10.1186/s13068-021-02030-9.

Giovannoni, M., Lironi, D., Marti, L., Paparella, C., Vecchi, V., Gust, A., Ferrari, S., 2021b. The Arabidopsis thaliana LysM-containing Receptor-Like Kinase 2 is required for elicitor-induced resistance to pathogens. Plant Cell Environ. 44 (12). https://doi.org/10.1111/pce.14192.

Giovannoni, M., Marti, L., Ferrari, S., Tanaka-Takada, N., Maeshima, M., Ott, T., Mattei, B., 2021c. The plasma membrane-associated Ca2+- binding protein PCaP1 is required for oligogalacturonide and flagellin-induced priming and immunity. Plant Cell Environ. https://doi.org/10.1111/pce.14118.

Giovannoni, M., Scafati, V., Rodrigues-Pousada, R.A., Benedetti, M., De Lorenzo, G., Mattei, B., 2024. The Vacuolar H+-ATPase subunit C is involved in oligogalacturonide (OG) internalization and OG-triggered immunity. Plant Physiol. Biochem. 216, 109117. https://doi.org/10.1016/j.plaphy.2024.109117.

Gravino, M., Locci, F., Tundo, S., Cervone, F., Savatin, D.V., De Lorenzo, G., 2017. Immune responses induced by oligogalacturonides are differentially affected by AvrPto and loss of BAK1/BKK1 and PEPR1/PEPR2. Mol. Plant Pathol. 18 (4), 582–595. https://doi.org/10.1111/mpp.12419.

Gray, D.-M., 2002. Improved Technology for dissolved oxygen measurement. In: 21st Annual Semiconductor Pure Water & Chemicals Conference Sponsored by Balazs AnalyticalServices/Air Liquide. Santa Clara, CA.

Heistinger, L., Gasser, B., Mattanovich, D., 2020. Microbe Profile: *Komagataella phaffii*: a methanol devouring biotech yeast formerly known as *Pichia pastoris*. Microbiology (Read.) 166 (7), 614–616. https://doi.org/10.1099/mic.0.000958.

Herzog, P., Sützl, L., Eisenhut, B., Maresch, D., Haltrich, D., Obinger, C., Peterbauer, C., 2019. Versatile oxidase and dehydrogenase activities of bacterial pyranose 2-oxidase facilitate redox cycling with manganese peroxidase *in vitro*. Appl. Environ. Microbiol. 85 (13), e00390. https://doi.org/10.1128/AEM.00390-19, 19.

Hwang, S., Lee, C.-H., Ahn, I.-S., 2008. Product identification of guaiacol oxidation catalyzed by manganese peroxidase. J. Ind. Eng. Chem. 14 (4), 487–492. https://doi.org/10.1016/j.jiec.2008.02.008.

Ichimura, K., Tena, G., Sheen, J., Henery, Y., Champion, A., Kreis, M., Zhang, S., Hirt, H., Wilson, C., Ellis, B.E., 2002. Mitogen-activated protein kinase cascades in plants: a new nomenclature. Trends Plant Sci. 7 (7). https://doi.org/10.1016/s1360-1385(02)02302-6.

Lee, M.-H., Lai, W.-L., Lin, S.-F., Hsu, C.-S., Liaw, S.-H., Tsai, Y.-C., 2005. Structural characterization of glucooligosaccharide oxidase from *Acremonium strictum*. Appl. Environ. Microbiol. 71 (12), 8881–8887. https://doi.org/10.1128/aem.71.12.8881-8887.2005.

Leferink, N.-G., Fraaije, M.-W., Joosten, H.-J., Schaap, P.-J., Mattevi, A., van Berkel, W.-J., 2009. Identification of a gatekeeper residue that prevents dehydrogenases from acting as oxidases. J. Biol. Chem. 284 (7), 4392–4397. https://doi.org/10.1074/jbc.M808202200.

Lever, M., 1972. A new reaction for colorimetric determination of carbohydrates. Anal. Biochem. 47, 273–279. https://doi.org/10.1016/0003-2697(72)90301-6.

Locci, F., Benedetti, M., Pontiggia, D., Citterico, M., Caprari, C., Mattei, B., De Lorenzo, G., 2019. An Arabidopsis berberine bridge enzyme-like protein specifically oxidizes cellulose oligomers and plays a role in immunity. Plant J. 98 (3), 540–554. https://doi.org/10.1111/tpj.14237.

Martinez-Medina, A., Flors, V., Heil, M., Mauch-Mani, B., Pieterse, C.M.J., Pozo, M.J., Conrath, U., 2016. Recognizing plant defense priming. Trends Plant Sci. 21 (10), 818–822. https://doi.org/10.1016/j.tplants.2016.07.009.

Mattevi, A., 2006. To be or not to be an oxidase: challenging the oxygen reactivity of flavoenzymes. Trends Biochem. Sci. 31 (5), 276–283. https://doi.org/10.1016/j.tibs.2006.03.003.

Mélida, H., Bacete, L., Ruprecht, C., Rebaque, D., Del Hierro, I., Lopez, G., Molina, A., 2020. Arabinoxylan-oligosaccharides act as damage associated molecular patterns in plants regulating disease resistance. Front. Plant Sci. 11, 1210. https://doi.org/10.3389/fpls.2020.01210.

Momeni, M., Fredslund, F., Bissaro, B., Raji, O., Vuong, T., Meier, S., M, A.H., 2021. Discovery of fungal oligosaccharide-oxidising flavo-enzymes with previously

unknown substrates, redox-activity profiles and interplay with LPMOs. Nat. Commun. 12 (1). https://doi.org/10.1038/s41467-021-22372-0.

Nühse, T.-S., Peck, S.-C., Hirt, H., Boller, T., 2000. Microbial elicitors induce activation and dual phosphorylation of the *Arabidopsis thaliana* MAPK 6. J. Biol. Chem. 275 (11), 7521–7526. https://doi.org/10.1074/jbc.275.11.7521.

Pontiggia, D., Benedetti, M., Costantini, S., De Lorenzo, G., Cervone, F., 2020. Dampening the DAMPs: how plants maintain the homeostasis of cell wall molecular patterns and avoid hyper-immunity. Front. Plant Sci. 11, 613259. https://doi.org/10.3389/fpls.2020.613259.

Puigbò, P., Guzmán, E., Romeu, A., Garcia-Vallvé, S., 2007. OPTIMIZER: a web server for optimizing the codon usage of DNA sequences. Nucleic Acids Res. 35 (Web Server issue). https://doi.org/10.1093/nar/gkm219.

Rolke, Y., Liu, S., Quidde, T., Williamson, B., Schouten, A., Weltring, K., Tudzynski, P., 2004. Functional analysis of H_2O_2-generating systems in *Botrytis cinerea*: the major Cu-Zn-superoxide dismutase (BCSOD1) contributes to virulence on French bean, whereas a glucose oxidase (BCGOD1) is dispensable. Mol. Plant Pathol. 5 (1). https://doi.org/10.1111/j.1364-3703.2004.00201.x.

Scafati, V., Troilo, F., Ponziani, S., Giovannoni, M., Scortica, A., Pontiggia, D., Benedetti, M., 2022. Characterization of two 1,3-β-glucan-modifying enzymes from *Penicillium sumatraense* reveals new insights into 1,3-β-glucan metabolism of fungal saprotrophs. Biotechnol. Biofuels Bioprod. 15 (1), 138. https://doi.org/10.1186/s13068-022-02233-8.

Scortica, A., Giovannoni, M., Scafati, V., Angelucci, F., Cervone, F., De Lorenzo, G., Mattei, B., 2022. Berberine Bridge Enzyme-Like oligosaccharide oxidases act as enzymatic transducers between microbial glycoside hydrolases and plant peroxidases. Molecular plant-microbe interactions : MPMI (Mol. PlanMolecular Plant-Microbe Interac.icrobe Interact.). https://doi.org/10.1094/MPMI-05-22-0113-TA.

Scortica, A., Scafati, V., Giovannoni, M., Benedetti, M., Mattei, B., 2023. Radical cation scavenging activity of berberine bridge enzyme-like oligosaccharide oxidases acting on short cell wall fragments. Sci. Rep. 13 (1), 4123. https://doi.org/10.1038/s41598-023-31335-y.

Spiro, M.D., Ridley, B.L., Eberhard, S., Kates, K.A., Mathieu, Y., O'Neill, M.A., Albersheim, P., 1998. Biological activity of reducing-end-derivatized oligogalacturonides in tobacco tissue cultures. Plant Physiol 116, 1289–1298. https://doi.org/10.1104/pp.116.4.1289.

Tonami, H., Uyama, H., Nagahata, R., Kobayashi, S., 2004. Guaiacol oxidation products in the enzyme-activity assay reaction by horseradish peroxidase catalysis. Chem. Lett. 33 (7), 796–797. https://doi.org/10.1246/cl.2004.796.

Tseng, Y.H., Scholz, S.S., Fliegmann, J., Krüger, T., Gandhi, A., Furch, A.C.U., et al., 2022. CORK1, A LRR-malectin receptor kinase, is required for cellooligomer-induced responses in *Arabidopsis thaliana*. Cells 11 (19), 2960. https://doi.org/10.3390/cells11192960.

Vuong, T.V., Vesterinen, A.H., Foumani, M., Juvonen, M., Seppälä, J., Tenkanen, M., Master, E.R., 2013. Xylo- and cello-oligosaccharide oxidation by gluco-oligosaccharide oxidase from *Sarocladium strictum* and variants with reduced substrate inhibition. Biotechnol. Biofuels 6, 148. https://doi.org/10.1186/1754-6834-6-148.

Zafred, D., Steiner, B., Teufelberger, A.-R., Hromic, A., Karplus, P.-A., Schofield, C.-J., Wallner, S., Macheroux, P., 2015. Rationally engineered flavin-dependent oxidase reveals steric control of dioxygen reduction. FEBS J. 282 (16), 3060–3074. https://doi.org/10.1111/febs.13212.

Zhang, Y., Dong, C., 2007. Regulatory mechanisms of mitogen-activated kinase signaling. Cell. Mol. Life Sci. : CM 64 (21). https://doi.org/10.1007/s00018-007-7012-3.